SUBVISUAL CIRRUS CLOUD PROPERTIES DERIVED FROM A FIRE IFO CASE STUDY

K. Sassen, M.K. Griffin and G.C. Dodd

Meteorology Department
University of Utah
Salt Lake City, UT 84112, U.S.A.

From the central Wisconsin IFO field site at Wausau, the University of Utah Mobile Polarization Lidar and a surface radiation station from the Lamont-Doherty Geological Observatory of Columbia University observed two very tenuous cirrus clouds on 21 October 1986. The clouds were present just below the height of the tropopause (12.78 km MSL), between -60 to -70°C. The first cloud was not detected visually, and is classified as subvisual cirrus. The second, a relatively narrow cloud band that was probably the remnants of an aircraft contrail, can be termed zenith-subvisual since, although it was invisible in the zenith direction, it could be discerned when viewed at lower elevation angles and also due to strong solar forward-scattering and corona effects. The observations provide an opportunity to assess the threshold cloud optical thickness associated with cirrus cloud visibility.

Ruby lidar (0.693 μm) backscattered signals were converted to isotropic volume backscatter coefficients (β, km^{-1} sr^{-1}) by applying the pure-molecular scattering assumption just below cloud base. The backscattering coefficient β_c due to the cloud is then obtained and expressed in relation to the molecular backscattering coefficient β_m in terms of the scattering ratio $R = (\beta_m + \beta_c)/\beta_m$. The linear depolarization ratio $\delta = \beta_\perp/\beta_\parallel$ for the cloud is computed after removing the essentially parallel-polarized scattering contributions from air molecules. The β_c values are also applied to determining the cloud optical thickness τ_c through the use of a backscatter-to-extinction ratio k, and the concentration of cloud particles using the backscattering gain g, and the effective diameter d_e of the particles obtained from the analysis of solar corona photographs. The sizes of the particles generating the corona are related to the angular separations between the centers of the red bands and the sun, as described in Sassen (1979), yielding diameters of ~25 μm. The direct and diffuse components of shortwave radiation fluxes (0.28-2.8 μm), measured by full hemispheric pyranometers, were used to compute the nadir optical thickness of the total atmosphere τ_t. Slight perturbations in the surface fluxes occurred during the cirrus passage, and the resultant variations in total optical thickness were equated with τ_c.

Given in Fig. 1 are lidar data in the form of height-versus-time displays of the scattering ratio R and linear depolarization ratio δ. To aid in the rejection of spurious data dominated by signal noise, 45-m (6 digitized data point) averages are used, a threshold of $R = 2.5$ is employed to define the cloud boundaries, and δ values are computed for $R \geq 5.0$. Both the structure and depolarizing properties of the subvisual (1545-1610) and zenith-subvisual (1625-

1700) cirrus clouds differ significantly. The former cloud displays a layered structure and low δ values, while the latter displays a concentric arrangement of scattering ratio contours and δ values more typical of cirrus. The appearance of the zenith-subvisual cloud is quite similar to that of long-lasting aircraft contrails. The weakly scattering layers that straddle the tropopause and extend into the lower stratosphere also appear to be composed of ice crystals.

The τ_c derived from the lidar and radiometric data are compared in Fig. 2, where the time scale of the radiometric data has been offset by 20 min to account for the advection time associated with cloud movement (at 16 m s^{-1}) between the zenith and solar elevation angles. (Note that local noon occurred at 1645 GMT). The two passive data records reflect the uncertainty in determining a "cloudless" optical thickness from the total atmospheric τ. The range of lidar-derived τ_c data values corresponds to the 0.05-0.10 range of k values considered appropriate for simple cirrus cloud particles. Although the cloud properties could be expected to display spatial and temporal variations, it is clear that both analysis methods yield comparable τ_c values. Given the inferred sizes of the cloud particles, which are relatively large in comparison to visible light wavelengths, differences between the broadband shortwave radiometric and monochromatic lidar data should not be significant.

Inferences about the microphysical composition of the zenith-subvisual cirrus cloud band can be drawn from combined photographic and lidar observations. Although the solar corona analysis reveals that the cloud particles must have been near-spherical and ~25 μm in diameter, the degree of lidar linear depolarization (Fig. 1) is consistent with hexagonal ice crystals, indicating that the thick-plate ice crystal habit (with axial ratios close to unity) was dominant. On the other hand, the subvisual cirrus probed prior to 1610 displayed much lower δ values and no optical phenomena, indicating differences in particle shapes and sizes. Compiled in Table 1 are the derived optical and microphysical quantities in terms of mean and maximum values for the subvisual and zenith-subvisual cirrus observation periods. The surface flux τ_c corresponds to the average of the two curves in Fig. 2, and the lidar data are derived for $k = 0.075$ and $g = 0.01$. The vertical depth of the cloud Δz is defined with respect to $R \geq 2.5$, and N_i and M_i represent the concentrations and ice mass contents of the clouds based on the 25 μm particle diameter estimate. In general, the microphysical properties of the zenith-subvisual cirrus are rather similar to those of an aircraft-sampled subvisual tropical cirrus (Heymsfield, 1986).

With regard to the zenith-subvisual cloud, which is of primary interest, a $\tau_c = 0.03$ value can be assigned as a threshold optical thickness for subvisual-versus-visual cirrus. This value compares favorably with the $\tau_c = 0.06$ reported by Platt et al. (1987) for a cirrus that was visible but very hazy in appearance. With regard to the $\tau_c = 0.03$ threshold value, it would appear that subvisual cirrus could have an impact on radiation transfer that is similar to the effects produced by the stronger episodes of stratospheric aerosol loading from volcanic eruptions or polar stratospheric clouds. Moreover, recent Stratospheric Aerosol and Gas Experiment (SAGE) satellite findings (Woodbury and McCormick, 1986) indicate that a category of optically thin cirrus, displaying extinction values at 1.0 μm between 8×10^{-4} to 8×10^{-3} km^{-1}, is fairly widespread on a global average. This extinction range is comparable to that obtained from

the β_c coefficients for our subvisual cirrus, suggesting that subvisual cirrus may represent a relatively significant component in the radiation balance of the earth-atmosphere system.

Acknowledgments. This research has been supported by NASA Grants NAG-1-686 and NAG-1-718, and by NSF Grant ATM-85 13975. The authors would like to thank D. Robinson of Lamont-Doherty Observatory for providing the surface radiation flux data.

References

Heymsfield, A.J., 1986: Ice particles observed in a cirriform cloud at -83°C and implications for polar stratospheric clouds. J. Atmos. Sci., 43, 851-855.

Platt, C.M.R., J.C. Scott and A.C. Dilley, 1987: Remote sounding of high clouds. Part VI: Optical properties of midlatitude and tropical cirrus. J. Atmos. Sci., 44, 729-747.

Sassen, K., 1979: Iridescence in an aircraft contrail. J. Opt. Soc. Am., 68, 1080-1083.

Woodbury, G.E. and M.P. McCormick, 1986: Zonal and geographical distributions of cirrus clouds determined from SAGE data. J. Geophys. Res., 91, 2775-2785.

Table 1. Mean and maximum (45 m-average) optical and microphysical properties for subvisual and zenith-subvisual cirrus derived from ruby lidar (0.694 μm) and surface shortwave (0.28-2.8 μm) flux data.

	Surface Flux	Lidar					Photographic + Lidar		
	τ_c	τ_c	R	β_c $(km\ sr)^{-1}$	Δz km	δ	d_e μm	N_i ℓ^{-1}	M_i $mg\ m^{-3}$
Subvisual Cirrus									
Mean	0.011	0.007	5.2	5.8×10^{-4}	0.77	0.19	--	---	---
Maximum	0.016	0.009	11.3	1.5×10^{-3}	1.00	----	--	---	---
Zenith-Subvisual Cirrus									
Mean	0.014	0.015	11.1	1.4×10^{-3}	0.65	0.35	25	25	0.2
Maximum	0.030	0.026	45.1	6.4×10^{-3}	0.95	----	25	110	0.9

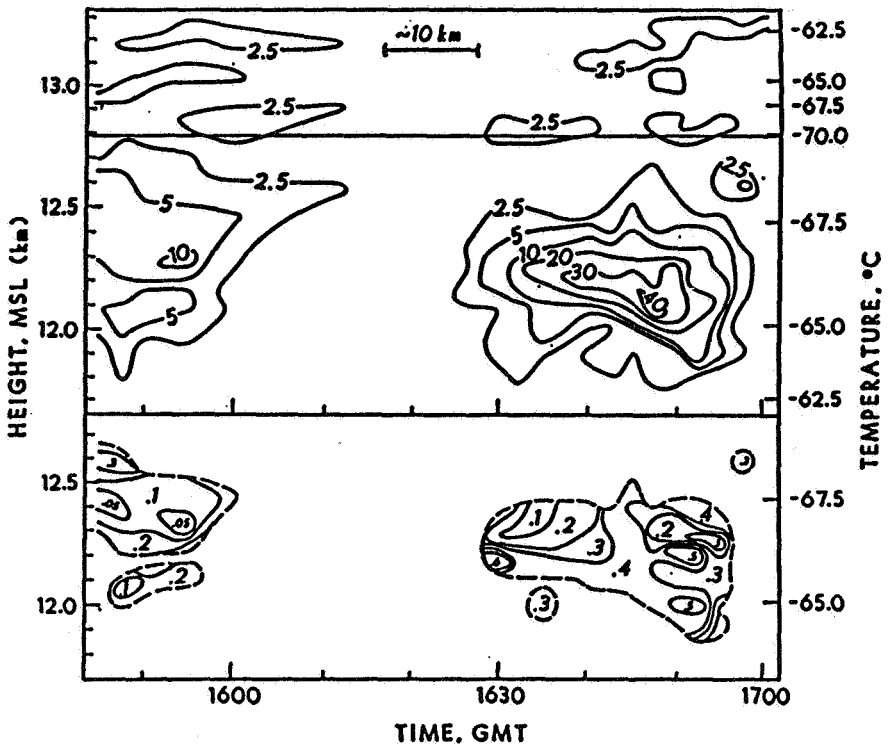

Fig. 1 Height-time displays of lidar scattering ratio R (top) and linear depolarization ratio δ (bottom) for the subvisual (prior to 1615) and zenith-subvisual cirrus clouds located just below the tropopause (line at 12.78 km).

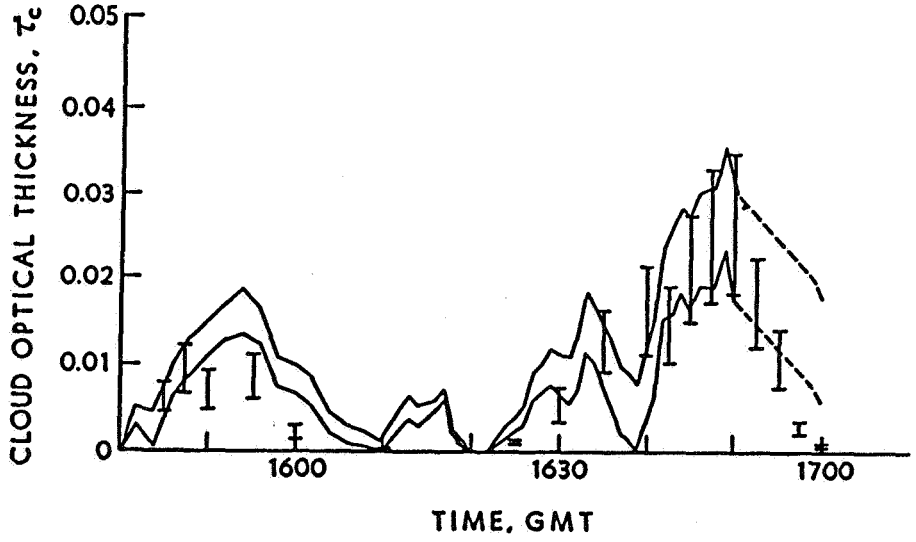

Fig. 2 Comparison of cloud optical thicknesses τ_c derived from lidar (bars for each shot) and surface shortwave radiation flux (continuous lines, for two approaches) during the passage of the cirrus. Dashed line segments correspond to a 9 min gap in the radiation records.